

Robustness and Generalization in Quantum Reinforcement Learning via Lipschitz Regularization

Nico Meyer^{1,2*}, Julian Berberich³, Christopher Mutschler¹, Daniel D. Scherer¹

¹Fraunhofer IIS, Fraunhofer Institute for Integrated Circuit IIS, Nürnberg, Germany.

²Pattern Recognition Lab, Friedrich-Alexander-Universität Erlangen-Nürnberg, Erlangen, Germany.

³University of Stuttgart, Institute for Systems Theory and Automatic Control, Stuttgart, Germany.

*Corresponding author. E-mail: nico.meyer@iis.fraunhofer.de;

Abstract

Quantum machine learning leverages quantum computing to enhance accuracy and reduce model complexity compared to classical approaches, promising significant advancements in various fields. Within this domain, quantum reinforcement learning has garnered attention, often realized using variational quantum circuits to approximate the policy function. This paper addresses the robustness and generalization of quantum reinforcement learning by combining principles from quantum computing and control theory. Leveraging recent results on robust quantum machine learning, we utilize Lipschitz bounds to propose a regularized version of a quantum policy gradient approach, named the RegQPG algorithm. We show that training with RegQPG improves the robustness and generalization of the resulting policies. Furthermore, we introduce an algorithmic variant that incorporates curriculum learning, which minimizes failures during training. Our findings are validated through numerical experiments, demonstrating the practical benefits of our approach.

Keywords: Quantum Computing, Reinforcement Learning, Control Theory, Lipschitz Regularization

1 Introduction

Quantum machine learning (QML) has emerged as a promising field at the intersection of quantum computing and of machine learning (Biamonte et al., 2017). It is conjectured to be a candidate for using noisy intermediate-scale quantum (NISQ) devices (Preskill, 2018) to realize quantum utility. Under specific conditions, it is known, that QML can unveil patterns intractable for classical methods. This enables exponential enhancements in model accuracy and convergence speed (Liu et al., 2021) for specific problem instances. With these advantages, QML is poised to revolutionize various domains, including optimization, cryptography, and drug discovery (Zaman et al., 2023).

Within the domain of QML, quantum reinforcement learning (QRL) has gained significant attention over recent years. This subfield lies at the intersection of

quantum computing, see Nielsen and Chuang (2011) for an introduction, and classical reinforcement learning (RL), as outlined by Sutton and Barto (2018). A comprehensive overview of QRL can be found in Meyer et al. (2022), highlighting some key challenges and approaches in the field. Often the central idea is to use a parametrized quantum circuit (PQC) (Cerezo et al., 2021) as a function approximator. Initially, there have been proposals to parameterize the Q-function (Chen et al., 2020; Skolik et al., 2022). Later papers extended the concept to direct parameterization of the policy (Jerbi et al., 2021; Meyer et al., 2023a), followed up by more sophisticated algorithmic variants (Wu et al., 2020; Yun et al., 2022). More recent work discusses offline QRL (Periyasamy et al., 2023), and the use of variational LSE solvers (Bravo-Prieto et al., 2023; Meyer et al., 2024) for quantum policy iteration (Meyer et al., 2024).

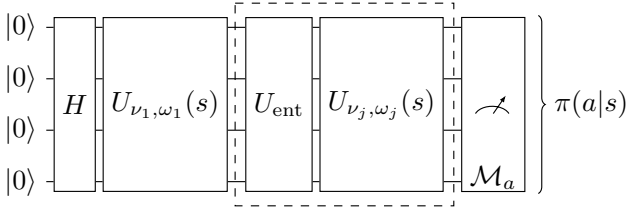


Fig. 1 The Quantum model used as the policy approximator in the proposed RegQPG algorithm. The parametrized unitaries are composed of single-qubit rotations with trainable variational weights ν_j and encoding parameters ω_j . This is followed by a static entanglement unitary and repeated several times. In the end, a tensored Pauli-Z observable is measured and plugged into Equation (18) to approximate the policy value.

When applying RL algorithms to complex and safety-critical applications ensuring reliable behavior becomes paramount. A key challenge is to cope with practical limitations such as noisy measurements or limited data samples, complicating the generalization from training data to unseen scenarios. In classical RL, generalization has received significant attention (Packer et al., 2019). Common approaches employ, e.g., robust policies which are insensitive to environment changes (Tamar et al., 2015) or adaptive policies which react to environment changes in a suitable way (Yu et al., 2017). In particular, the generalization capability of a policy can be quantified in terms of its Lipschitz continuity properties (Wang et al., 2019).

Our paper contributes to the field of QRL as follows: We modify the training procedure of quantum policy gradients (QPG) with additional Lipschitz-based regularization, dubbed regularized quantum policy gradients (RegQPG). The underlying theory is derived in Section 2, and the experimental setup used in this paper is described in Section 3. We formulate and quantify the robustness of the respective trained QRL policies in Section 4. Our findings indicate, that RegQPG enhances the robustness over a wide range of state perturbation strengths. Furthermore, we extend our analysis to consider generalization capabilities in Section 5. The results in Section 5.1 show a clearly enhanced generalization performance over different ranges of initial conditions when using Lipschitz regularization. Moreover, the extension with concepts from curriculum learning in Section 5.2 – dubbed curriculum regularized quantum policy gradients (CurrRegQPG) – further improves these generalization capabilities, while also minimizing the number of failures during training. Finally, Section 6 discusses the significance of our findings for the QRL community, proposes future extensions, and concludes the paper.

2 Regularized QRL Training

We consider a common RL setup, where the action $a \in \mathcal{A}$ is determined via a parameterized policy

$$a \sim \pi_{\Theta}(a|s), \quad (1)$$

with $\sum_a \pi_{\Theta}(a|s) = 1$. Here, $s \in \mathcal{S} \subseteq \mathbb{R}^n$ denotes the environment state, $a \in \mathcal{A}$ is an action from a discrete set, and Θ summarizes the trainable parameters. We furthermore introduce the notion

$$\pi_{\Theta}(\cdot|s) = [\pi_{\Theta}(a = 0|s), \pi_{\Theta}(a = 1|s), \dots], \quad (2)$$

mapping the environment state to the space of probability distributions over the actions. Our goal is to iteratively adapt the parameters Θ to maximize the cumulative and discounted return

$$J(\Theta) = \sum_{t'=t}^{T-1} \gamma^{t'-t} r_{t'} \quad (3)$$

for some horizon T and discount factor $0 \leq \gamma \leq 1$. Note that the reward r_t depends on the evolution of the state s_t under the action sampled from $\pi_{\Theta}(s_t)$ as well as the action a_t itself, which is why $J(\Theta)$ is a function of the parameters Θ . Further details on the concept of RL can be found in Sutton and Barto (2018).

In this paper, we use a PQC to approximate the policy π_{Θ} . More specifically, π_{Θ} is represented by a quantum model with variational parameters, in particular including a trainable encoding (Berberich et al., 2023). This can be expressed as

$$\pi_{\Theta}(a|s) = \langle 0|U_{\Theta}(s)^{\dagger} \mathcal{P}_a U_{\Theta}(s)|0\rangle, \quad (4)$$

with some projector \mathcal{P}_a and parametrized quantum circuit $U_{\Theta}(s)$. For the policy to form a probability distribution over the actions, we furthermore require that $\sum_a \mathcal{P}_a = \mathbb{1}$ and $\mathcal{P}_a \mathcal{P}_{a'} = \delta_{a,a'} \mathcal{P}_a$. The latter is defined as

$$U_{\Theta}(s) = U_{N, \Theta_N}(s) \cdots U_{1, \Theta_1}(s) \quad (5)$$

for layers $j = 1, \dots, N$ and unitary operators

$$U_{j, \Theta_j}(s) = e^{-i(\nu_j + \omega_j^{\top} s) H_j}, \quad (6)$$

More precisely, we train a policy that not only maximizes the return $J(\Theta)$ but also admits a small Lipschitz bound. Mathematically, a Lipschitz bound of a function f is any number $L > 0$ such that

$$\|f(x) - f(x')\| \leq L \|x - x'\| \quad (7)$$

holds for any (x, x') . For each action a , a Lipschitz bound on the PQC (4) can be derived as

$$L_{\Theta, a} = 2\|\mathcal{P}_a\| \sum_{j=1}^N \|\omega_j\| \|H_j\|, \quad (8)$$

for details see Berberich et al. (2023). This implies the following Lipschitz bound for the vector of probability distributions (2)

$$L_{\Theta} = \sum_a L_{\Theta, a} = \sum_a 2\|\mathcal{P}_a\| \sum_{j=1}^N \|\omega_j\| \|H_j\|. \quad (9)$$

In the context of RL, a small Lipschitz bound implies robustness of the policy against input perturbations, which may, e.g., arise due to noisy measurements of the state s_t (see Section 4); further, a small Lipschitz bound enhances the generalization of the policy over varying initial conditions, both during and after training (see Section 5). Motivated by these facts, in this paper, we solve a multiobjective optimization problem: maximize $J(\Theta)$ while keeping L_{Θ} small. Note that the Lipschitz bound depends directly on the norm of the trainable parameters ω_j . Thus, we define a regularized reward function which encodes these two objectives

$$J_{\text{reg}(\lambda)}(\Theta) = J(\Theta) - \lambda \sum_{j=1}^N \|\omega_j\|^2 \|H_j\|^2, \quad (10)$$

where $\lambda \geq 0$ is a hyperparameter which can be tuned by the user, e.g., via cross-validation. Larger values of λ encourage a more robust and stabilizing policy at the price of a possibly reduced reward $J(\Theta)$. We train the policy via gradient ascent

$$\Theta \leftarrow \Theta + \alpha \nabla_{\Theta} J_{\text{reg}(\lambda)}(\Theta), \quad (11)$$

resulting in a so-called *policy gradient* approach (Sutton et al., 1999). The gradient of the regularized objective is obtained by

$$\nabla_{\Theta} J_{\text{reg}(\lambda)}(\Theta) = \nabla_{\Theta} J(\Theta) - \nabla_{\Theta} \left(\lambda \sum_{j=1}^N \|\omega_j\|^2 \|H_j\|^2 \right), \quad (12)$$

where $\nabla_{\Theta} J(\Theta)$ can be estimated with the *policy gradient theorem* (Sutton et al., 1999). This concept has already been generalized to *quantum policy gradients* in previous work (Jerbi et al., 2021; Meyer et al., 2023a). Note that the regularization causes an additional linear term in the update of the trainable encoding

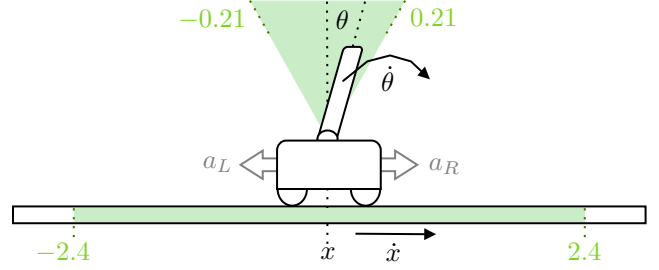


Fig. 2 Sketch of **CartPole** environment, see also Table 1 for details on observations.

Table 1 Observations from the **CartPole** environment, refer also to Figure 2 for sketch. We report the admissible *range* of observations, the corresponding *initial* conditions, the factor we use to *normalize* to the approximate range $[-1, 1]$ for encoding, and the *unit* in which the quantities are measured.

	Cart		Pole	
	Position x	Velocity \dot{x}	Angle θ	Velocity $\dot{\theta}$
Range	$[-2.4, 2.4]$	$[-\infty, \infty]$	$[-0.21, 0.21]$	$[-\infty, \infty]$
Initial	all uniform at random in range $[-0.05, 0.05]$ ¹			
Norm	2.4	2.5	0.21	2.5
Unit	m	m/s	rad	rad/s

¹Standard setting of initial conditions for **CartPole** environment, refers to unnormalized observations.

parameters ω_j , i.e.,

$$w_j \leftarrow w_j + \alpha \nabla_{\omega_j} J(\Theta) - 2\alpha\lambda \|\omega_j\|^2 \omega_j. \quad (13)$$

Since the Lipschitz bound (9) is independent of the parameters ν_j , the update of the *standard* variational parameters ν_j 's is not influenced by the regularization. Due to the main components of the proposed routine, we furthermore refer to it as the regularized quantum policy gradients (RegQPG) algorithm. In the remainder of the paper, we study the impact of the above regularization on robustness (Section 4) and generalization (Section 5) of the trained policy (Section 5.1). Furthermore, we develop a variant based on curriculum learning to further improve generalization and minimize the number of failures during training in (Section 5.2), dubbed the CurrRegQPG algorithm.

3 Experimental Setup

In the following, we will describe the detailed algorithmic specifications and hyperparameter setting used for training the QRL agents, and for all experiments in Sections 4 and 5 building upon this. All implementations were realized using the `qiskit-torch-module` (Meyer et al., 2024), an extension of the Qiskit library (Javadi-Abhari et al., 2024) for

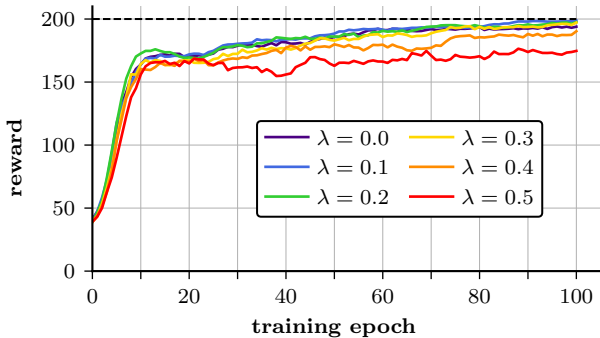


Fig. 3 Training using the RegQPG algorithm on the `CartPole` environment. One epoch performs updates on trajectories from 10 environment instances. The strength of Lipschitz regularization is indicated by λ . Training performance is averaged over 100 random seeds.

the fast training of quantum neural networks. A repository supporting full reproducibility of the results can be accessed as noted in the code availability statement.

The used PQC is a modified version of an ansatz frequently employed in QPG algorithms (Jerbi et al., 2021; Meyer et al., 2023a,b) and is sketched in Figure 1. It includes variational parameters ν and trainable encoding parameters ω , satisfying Equations (5) and (6). After an initially created equal superposition, parameterized unitaries $U_{\nu_j, \omega_j}(s)$ and all-to-all Pauli-Z entanglement unitaries U_{ent} are applied in alternation:

$$U_{\nu, \omega}(s) = U_{\nu_L, \omega_L}(s) \cdots U_{\text{ent}} U_{\nu_1, \omega_1}(s) H^{\otimes n} |\mathbf{0}\rangle \quad (14)$$

Hereby, L denotes the number of layers – we use $L = 3$ for all experiments. The individual parameterized unitaries are composed as

$$U_{\nu_j, \omega_j}(s) = U_{\nu_j} U_{\omega_j}(s), \quad j = 1, 2, \dots, L, \quad (15)$$

where we implement the state-independent and state-dependent parts individually using single-qubit rotations, i.e.,

$$U_{\nu_j} = \bigotimes_i R_y(\nu_{j,i,1}) R_z(\nu_{j,i,0}) \quad (16)$$

$$U_{\omega_j}(s) = \bigotimes_i R_z(\omega_{j,i,1} \cdot s_i) R_z(\omega_{j,i,0} \cdot s_i). \quad (17)$$

This formulation is an instance of the more general version in Equations (5) and (6). This could be seen by replacing the $\omega_{j,i,k}$, with one-hot encoded vectors, i.e., $[0, \dots, \omega_{j,i,k}, \dots, 0]^t s = \omega_{j,i,k} \cdot s_i$, with $k = 0, 1$. In the context of (quantum) policy gradients, we employ a stochastic policy $\pi(a|s) \mapsto [0, 1]$, with $\sum_a \pi(a|s) = 1$. For two actions $a = \{0, 1\}$, we can use the explicit

definition

$$\pi(a|s) = \frac{(-1)^a \cdot \langle U_{\nu, \omega}(s)^\dagger | Z^{\otimes n} | U_{\nu, \omega}(s) \rangle + 1}{2}, \quad (18)$$

which by Born’s rule is guaranteed to be a valid probability density function. There also exist extensions to larger action spaces (Meyer et al., 2023a).

For experimentally validating the claims in this paper, we use the `CartPole` environment (Brockman et al., 2016), sketched in Figure 2. The task is to balance a pole mounted on a car by steering it left or right while avoiding violating spatial or angular conditions. Details on admissible values for the entries of the four-dimensional state are summarized in Table 1. For encoding into the PQC, the entries are normalized to the range $[-1, 1]$, where the normalization factors for velocity \dot{x} and angular velocity $\dot{\theta}$ hold for typically encountered values. A reward of $r = 1$ is given for each successful timestep, with a horizon of $T = 200$. During training, the rewards are discounted with a factor $\gamma = 0.99$ following Equation (3). As the state is four-dimensional, an instance with $n = 4$ qubits of the ansatz defined in Equations (15) to (17) is used.

We trained with the described setup for 100 epochs, each performing updates on a batch of 10 full trajectories, using a learning rate of $\alpha = 0.05$. The results for different regularization rates λ – following the procedure described in Section 2 – are shown in Figure 3. All curves are averaged over 100 random seeds. The training converges to a near-optimal policy in the absence of regularization (i.e., $\lambda = 0.0$), and for regularization rates $\lambda = \{0.1; 0.2; 0.3\}$, with no significant differences in convergence behavior. For a higher regularization rate of $\lambda = 0.4$, and especially $\lambda = 0.5$, the procedure does not converge to the optimal reward of 200, since the regularization outweighs the reward, compare Section 2. In Section 4 and Section 5, we demonstrate that the proposed regularization significantly improves the robustness and generalization of the learned policy.

4 Robustness of QRL Policies

By definition, a Lipschitz bound of the policy π_Θ quantifies robustness against perturbed state measurements. To be precise, suppose that instead of the true state s only a perturbed measurement $\tilde{s} = s + \varepsilon$ is available, e.g., due to measurement noise or an adversarial attack (Goodfellow et al., 2014; Szegedy et al., 2014). Then, due to (7), the change of the policy π_Θ is bounded as

$$\|\pi_\Theta(\cdot|\tilde{s}) - \pi_\Theta(\cdot|s)\| \leq L_\Theta \|\varepsilon\|. \quad (19)$$

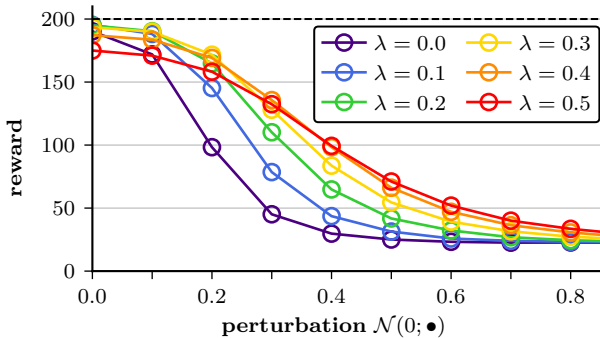


Fig. 4 Lipschitz regularization enhances robustness of policies trained with the RegQPG algorithm. The models from Figure 3 are tested on modified `CartPole` environments with observation perturbation, i.e. additive zero-mean Gaussian noise with increasing variance. Testing performance is averaged over 100 random seeds for each model, resulting in 10000 samples contributing to each data point.

Thus, a smaller Lipschitz bound L_{Θ} implies an improved worst-case robustness against (additive) state perturbations.

In Figure 4, we demonstrate that the regularized training strategy proposed in Section 2 does indeed significantly improve the robustness of the trained policy. To this end, we assumed that the observations are perturbed with zero-mean Gaussian noise of increasing variance. The noise value is sampled from the respective distribution and applied to each element of the four-dimensional state individually. This happens after observation normalization as noted in Table 1, i.e., the offset is applied to values in the approximate range $[-1, 1]$. It is important to note that the actual state of the environment is not affected by that perturbation.

We test all 100 trained policies for each regularization rate from Section 2 on 100 instances of the described `Perturbed CartPole` environment, for perturbation strengths ranging from $\mathcal{N}(0; 0.0)$ (i.e. no perturbation) to $\mathcal{N}(0; 0.8)$. As expected, for each trained policy, the obtained reward decreases with increasing perturbation. In particular, the performance drops to a value of about 25. This is the performance of a basically random agent on the `CartPole` environment, which can be explained by the observations being so noisy, that no informed decisions can be made. Further, while small regularization parameters $\lambda = \{0.0; 0.1; 0.2; 0.3\}$ correspond to the same optimal performance obtained during training in the absence of noise, significant differences can be observed for increasing noise levels. In particular, Figure 4 shows a direct correlation between higher regularization parameters λ (i.e., smaller Lipschitz bounds of the trained

policies) and higher reward for non-trivial noise levels. On the other hand, too high regularization, e.g., $\lambda = 0.5$, leads to a substantially lower reward for small noise levels since the regularized reward function (10) is unnecessarily biased towards overly robust solutions.

Notably, a sweet spot can be observed for regularization with $\lambda = 0.3$, for which a substantially higher reward can be obtained than in the case without regularization (i.e. $\lambda = 0.0$) across all considered noise levels. Overall, we can conclude, that Lipschitz regularization, as implemented in RegQPG, can significantly improve the robustness of quantum policies.

5 Generalization of QRL Policies

In this section, we study the impact of Lipschitz regularization on the generalization of QRL policies. In particular, we show that Lipschitz regularization improves the ability of QRL policies to reliably control the underlying system even for initial states not included in the training data. Intuitively, a small Lipschitz bound ensures that the policy π_{Θ} does not change too rapidly for varying states and, therefore, effects of overfitting are reduced. While this connection is well-known in classical supervised machine learning (Xu and Mannor, 2012) and has recently been explored in supervised QML (Berberich et al., 2023), our results in this section exploit it for the first time in QRL. In particular, in Section 5.1, we show that Lipschitz regularization indeed increases the region in which failure-free operation can be ensured after training. Next, in Section 5.2, we incorporate curriculum learning ideas for exploring the state space, which further improves generalization and minimizes the number of failures during training.

5.1 Generalization of Trained Policies

We experimentally support the claim that Lipschitz regularization enhances the generalization capabilities of trained policies in Figure 5. For this, we evaluated the *attraction rate* of the policies trained in Section 2 with regularization rates $\lambda = \{0.0; 0.1; 0.2; 0.4\}$ – for a definition see below. We found the pole angle to be the factor that much more frequently causes failed episodes, as opposed to the cart position. Therefore, we focus our analysis on the initial conditions for the pole, rather than the spatial factors. In particular, we evaluated initial conditions for the pole angular velocity sampled uniformly at random in $[0.00, 0.02]$, $[0.02, 0.04]$, \dots , $[0.24, 0.26]$, and pole angles sampled uniformly at random in $[-2.75, -2.25]$, $[-2.25, -1.75]$, \dots , $[2.25, 2.75]$. Note, that all those values are successively normalized following Table 1, before being provided as initial observations to the agent. We evaluate the generalization

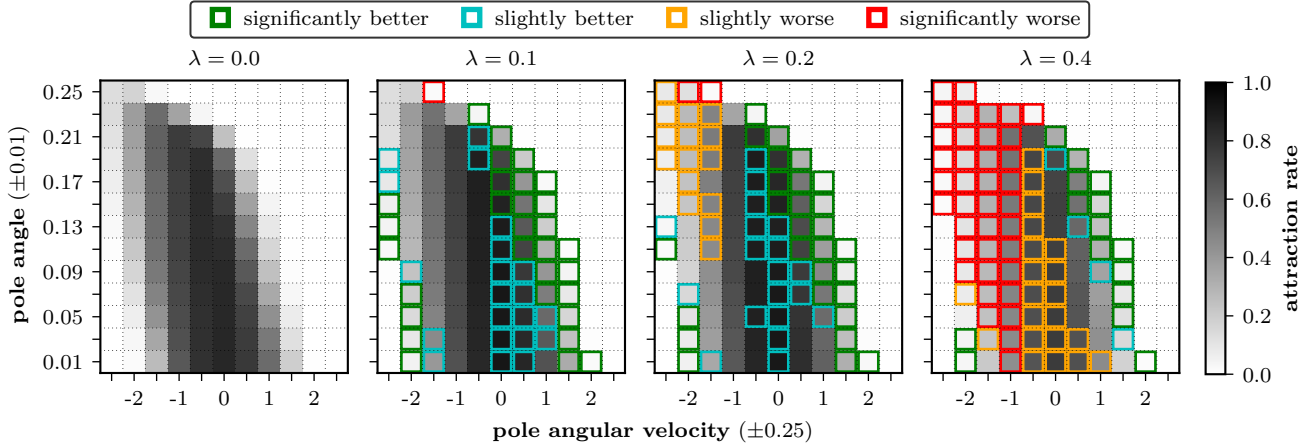


Fig. 5 Lipschitz regularization enhances generalization of policies trained with the RegQPG algorithm. During training, all features – cart position, cart velocity, pole angle, pole angular velocity – are by default initialized randomly at uniform in $[-0.05, 0.05]$. We test on a wider range of pole angles and angular velocities, and report the rate of attraction for these configurations, i.e. the fraction of successful test runs – see also Equation (20). The 100 models for each regularization rate are evaluated for 100 runs each, i.e. 10000 samples contribute to each data point. Regions where the policies obtained via regularized training deviate from the non-regularized baseline and their corresponding full (half) confidence intervals – defined by the variances – do not overlap are highlighted as significantly (slightly) better or worse, respectively.

over different initial conditions in terms of the *attraction rate*, which quantifies the fraction of succeeded test runs. More formally, for a reward of $r = +1$ for each successful step, this reads:

$$\frac{1}{\text{runs}} \cdot \delta_{T=\sum_i^T r_i} \quad (20)$$

Hereby, δ is an indicator function, that evaluates to 1, iff the run has achieved the maximal reward. In the considered setup, the horizon is $T = 200$, and 100 runs were performed for each setup.

The first thing one might notice about Figure 5 is that the results are not mirrored along the zero pole angular velocity axis. This is caused by negative velocities potentially offsetting large positive angles in the successive steps, while matters only get worse for positive velocities. However, the results are approximately point symmetrical (w.r.t the all-zero position) for negative angles, which we have skipped to avoid clustering of the plots. To simplify the interpretation of the results, we marked cells for which the regularized versions are more or less stable than the non-regularized baseline. We consider a setup to be *considerable* better (or worse) if the standard deviations – computed over all 100 models – do not overlap. If only the halved standard deviations do not overlap, we consider this to be a *slightly* better (or worse) performance.

A regularization rate of $\lambda = 0.1$ improves the generalization compared to the non-regularized baseline on various initial conditions. However, the gain is especially pronounced for positive angular velocities. This trend is continued for $\lambda = 0.2$, where even larger

improvements for positive velocities can be reported, while the performance deteriorates slightly for negative velocities. This can be explained by the regularization during training limiting the impact of state input on the model output, which also includes the signs of values. For certain tasks, one might only want to *regularize* certain properties of the state. This could be done e.g. by encoding the state magnitude and state sign separately, while only applying regularization to the parameters associated with the former one. However, such extensions are left for future work. For a high regularization rate of $\lambda = 0.4$, apart from some exceptions, the trained models are less stable than the baseline. This is expected behavior, as too large regularization rates tend to obstruct the overall performance. Overall, depending on what regions the policy acts, a regularization rate between $\lambda = 0.1$ and $\lambda = 0.2$ is optimal for the considered setup.

5.2 Incorporating Curriculum Learning

While Section 5.1 aimed at training policies that generalize well after training, we now additionally want to minimize the number of failures during training. To this end, we propose the curriculum regularized quantum policy gradients (CurrRegQPG) approach in Algorithm 1, which closely resembles the concept of curriculum learning from classical RL (Elman, 1993; Rohde and Plaut, 1999). It incorporates three core concepts: (i) a standard quantum policy gradients approach, as proposed in Meyer et al. (2023a); (ii) a regularization strategy based on Lipschitz bounds, as described in Section 2, and analyzed regarding generalization in the

Algorithm 1 Curriculum Reg. QPG (CurrRegQPG)

Input: policy approximator π , learning rate α , regularization rate λ , maximum number of failures f_{\max} , increasing range of initial conditions r_1, r_2, \dots, r_m
Output: increasingly general policies $\pi_{r_1}^*, \pi_{r_2}^*, \dots$

Initialize parameters, e.g. $\nu \sim [-\pi, \pi]$, $\omega \sim \mathcal{N}(0; 0.1)$
Initialize failure counter $f \leftarrow 0$
Select first range of initial conditions $r \leftarrow r_1$
while Number of failures $f < f_{\max}$ **do**
 Sample initial state s_1 from range r
 Follow policy $\pi_{\Theta=\{\nu, \omega\}}: s_1, a_1, r_1, \dots, s_T, a_T, r_T$
 if Episode lead to failure **then**
 Increase failure counter $f \leftarrow f + 1$
 end if
 if Validation generalizes on range r **then**
 if Reached final range $r = r_m$ **then**
 Store $\pi_{r_m}^* \leftarrow \pi_{\Theta}$ and terminate
 end if
 Select next range $r (= r_i) \leftarrow r_{i+1}$
 Store intermediate policy $\pi_{r_i}^* \leftarrow \pi_{\Theta}$
 end if
 Update $\Theta \leftarrow \Theta + \alpha \nabla_{\Theta} J_{\text{reg}(\lambda)}(\Theta)$, see Eq. 12
end while

previous paragraphs; (iii) an incrementally increasing range of initial conditions, intended to minimize the probability of failures, similar to Berkenkamp et al. (2017); The algorithm initially trains on a small range of initial conditions, and keeps track of the number of failures – i.e. validating conditions on either angle or spatial coordinates for `CartPole` – during this process. Validation is performed to determine if the policy sufficiently generalizes over current range. If this is the case, the range of initial conditions is increased. This procedure continues until either the maximum number of failures has been reached, or generalization on the final range has been achieved. While this does not guarantee that no failures occur during training, the number can be significantly reduced in the presence of regularization, as we demonstrate in the following.

For our proof-of-concept realization, we concentrated on incrementally enlarging the range of initial conditions for the pole angular velocity. We assert validation to be successful, if the average reward over 100 runs exceeds 195 – i.e. the default termination condition for the `CartPole` environment. Moreover, we set a cut-off after at most 1000 failures, and increased ranges from $[-0.25, 0.25]$ to $[-1.75, 1.75]$ in four steps. We report the empirical results in Table 2. The results indicate, that for a regularization rate of $\lambda = 0.1$, the number of failures required for the policy to generalize over all ranges is reduced, compared to the

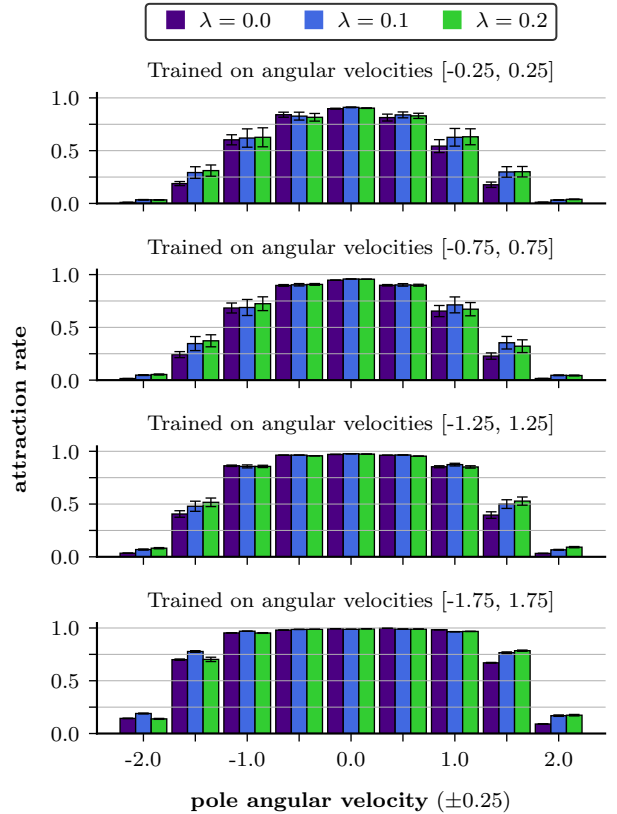


Fig. 6 Generalization of policies for the models trained with CurrRegQPG on increasing ranges of initial conditions from Table 2. The results are averaged only over the converged training runs, with the error bars denoting the standard deviations. The generalization was evaluated for 100 test runs each, i.e. up to 10000 samples contribute to each data point.

Table 2 Lipschitz regularization minimizes number of failures during training of policies with the CurrRegQPG algorithm. We consider increasing ranges of initial conditions for the pole angular velocity, while all other state elements are initialized following the default procedure in Table 1. We report the average number of failures that occurred during training to ensure generalization over the respective range, with the maximum number of failures set to 1000. Furthermore, we note the fraction of runs – out of 100 – that was able to guarantee generalization over the respective configuration.

Failures	$\lambda = 0.0$	$\lambda = 0.1$	$\lambda = 0.2$
$[-0.25, 0.25]$	208.9	178.3	167.9
$[-0.75, 0.75]$	280.4	228.3	228.3
$[-1.25, 1.25]$	479.1	394.6	489.0
$[-1.75, 1.75]$	990.8	762.5	952.8
Converged	$\lambda = 0.0$	$\lambda = 0.1$	$\lambda = 0.2$
$[-0.25, 0.25]$	99%	100%	100%
$[-0.75, 0.75]$	97%	100%	100%
$[-1.25, 1.25]$	83%	85%	78%
$[-1.75, 1.75]$	3%	41%	8%

non-regularized baseline. Moreover, especially the fraction of runs that were able to achieve generalization over the final range $[-1.75, 1.75]$ significantly increases from 3% to 41% in the presence of regularization. For a larger regularization rate of $\lambda = 0.2$, one can still observe a small advantage compared to the baseline on the larger ranges, but the difference is much less significant.

To provide more insights into the actually learned policies, we evaluated the generalization behavior at the intermediate steps in Figure 6. The plots only present data from the actually terminated runs, which leads to only small differences between the models. However, one can identify a similar pattern as in Figure 5, i.e. the regularized models better generalize over initial conditions not explicitly trained on. Moreover, the worse generalization for $\lambda = 0.2$ on negative vs. positive angular velocities explains the overall worse performance during cautious training. In general, the CurrRegQPG algorithm can enhance the generalization of policies on the desired ranges. A note regarding this, as especially for the bottom plot there are some bars with an attraction rate of only approx. 0.75: validation in CurrRegQPG determines success as reaching an average reward of 195 over 100 runs, which means that several instances could have fallen short of reward 200; generalization is evaluated as the fraction of runs that have reached reward 200, i.e. a stricter condition; Overall, a regularization rate of $\lambda = 0.1$ seems to be an optimal parameter for the CurrRegQPG algorithm in the considered setup.

6 Discussion

In this paper, we have explored the robustness and generalization capabilities of quantum reinforcement learning (QRL) by integrating principles from quantum computing, classical RL, and control theory. Our primary contribution is the development of the regularized quantum policy gradients (RegQPG) algorithm. It leverages Lipschitz bounds to enhance the robustness and generalization of QRL policies. Additionally, we proposed the curriculum regularized quantum policy gradients (CurrRegQPG) approach to reduce the number of failures during training. Our numerical experiments demonstrated the effectiveness of the RegQPG and CurrRegQPG algorithms.

One of the key strengths of the proposed methods is their computational efficiency. Applying the regularization is computationally cheap, making it feasible to implement these strategies in various scenarios and applications. This efficiency is particularly important considering the scarcity of quantum computing resources, especially in the NISQ era.

Future work should consider less conservative conditions than those based on the Lipschitz bound in Equation (9). While the Lipschitz bound provides a solid foundation for ensuring robustness, it may limit the performance of QRL policies in certain scenarios. Exploring alternative conditions that balance robustness and performance more effectively could circumvent this. Furthermore, it might be interesting to investigate the integration of these regularization methods with QRL algorithms beyond quantum policy gradients.

Finally, our work provides the basis for studying safety of QRL algorithms. In classical RL, safety has been extensively studied (Gu et al., 2022). Various methods have been proposed, such as safe RL via Lyapunov methods and related approaches (Berkenkamp et al., 2017; Chow et al., 2018; Dawson et al., 2023). In these approaches, guarantees are often provided by restricting the Lipschitz bound of the policy, as demonstrated in Berkenkamp et al. (2017); Dawson et al. (2023). Lipschitz regularization in RL has also been explored in Berkenkamp et al. (2017); Bjorck et al. (2021); Gogianu et al. (2021); Takase et al. (2022), highlighting the important role that the Lipschitz bound plays. Likewise, we expect that our framework paves the way for studying safety in QRL.

In summary, this paper has made significant strides in enhancing the robustness and generalization capabilities of QRL by incorporating Lipschitz bounds. Our findings underscore the importance of efficient regularization techniques and open new avenues for future research to expand the applicability of QRL in the real world.

Code Availability

Implementations of the RegQPG and CurrRegQPG algorithms are available in the repository <https://github.com/nicomeyer96/regularized-qpg>. The framework allows for full reproducibility of the experimental results in this paper by executing a single script. Usage instructions and additional details can be found in the README file. Further information and data is available upon reasonable request.

Acknowledgments

NM acknowledges support by the Bavarian Ministry of Economic Affairs, Regional Development and Energy with funds from the Hightech Agenda Bayern via the project BayQS. JB acknowledges funding by Deutsche Forschungsgemeinschaft (DFG, German Research Foundation) under Germany’s Excellence Strategy - EXC 2075 - 390740016 and the support by the Stuttgart Center for Simulation Science (SimTech).

References

- Brockman, G., Cheung, V., Pettersson, L., Schneider, J., Schulman, J., Tang, J., Zaremba, W.: OpenAI Gym. arXiv:1606.01540 (2016)
- Berberich, J., Fink, D., Pranjić, D., Tutschku, C., Holm, C.: Training robust and generalizable quantum models. arXiv:2311.11871 (2023)
- Bjorck, N., Gomes, C.P., Weinberger, K.Q.: Towards deeper deep reinforcement learning with spectral normalization. In: *Advances in Neural Information Processing Systems*, vol. 34, pp. 8242–8255 (2021)
- Bravo-Prieto, C., LaRose, R., Cerezo, M., Subasi, Y., Cincio, L., Coles, P.J.: Variational quantum linear solver. *Quantum* **7**, 1188 (2023)
- Berkenkamp, F., Turchetta, M., Schoellig, A., Krause, A.: Safe model-based reinforcement learning with stability guarantees. In: *Advances in Neural Information Processing Systems*, pp. 908–918 (2017)
- Biamonte, J., Wittek, P., Pancotti, N., Rebentrost, P., Wiebe, N., Lloyd, S.: Quantum machine learning. *Nature* **549**(7671), 195–202 (2017)
- Cerezo, M., Arrasmith, A., Babbush, R., Benjamin, S.C., Endo, S., Fujii, K., McClean, J.R., Mitarai, K., Yuan, X., Cincio, L., Coles, P.J.: Variational quantum algorithms. *Nat. Rev. Phys.* **3**, 625–644 (2021)
- Chow, Y., Nachum, O., Duenez-Guzman, E., Ghavamzadeh, M.: A lyapunov-based approach to safe reinforcement learning. In: *Advances in Neural Information Processing Systems*, vol. 31 (2018)
- Chen, S.Y.-C., Yang, C.-H.H., Qi, J., Chen, P.-Y., Ma, X., Goan, H.-S.: Variational quantum circuits for deep reinforcement learning. *IEEE Access* **8**, 141007–141024 (2020)
- Dawson, C., Gao, S., Fan, C.: Safe control with learned certificates: A survey of neural lyapunov, barrier, and contraction methods for robotics and control. *IEEE Trans. Robotics* **39**(3), 1749–1767 (2023)
- Elman, J.L.: Learning and development in neural networks: The importance of starting small. *Cognition* **48**(1), 71–99 (1993)
- Gogianu, F., Berariu, T., Rosca, M.C., Clopath, C., Busoniu, L., Pascanu, R.: Spectral normalisation for deep reinforcement learning: An optimisation perspective. In: Meila, M., Zhang, T. (eds.) *Proc. 38th Int. Conf. Machine Learning (ICML)*, vol. 139, pp. 3734–3744 (2021)
- Goodfellow, I.J., Shlens, J., Szegedy, C.: Explaining and harnessing adversarial examples. arXiv:1412.6572 (2014)
- Gu, S., Yang, L., Du, Y., Chen, G., Walter, F., Wang, J., Knoll, A.: A review of safe reinforcement learning: Methods, theory and applications. arXiv:2205.10330 (2022)
- Javadi-Abhari, A., Treinish, M., Krsulich, K., Wood, C.J., Lishman, J., Gacon, J., Martiel, S., Nation, P.D., Bishop, L.S., Cross, A.W., Johnson, B.R., Gambetta, J.M.: Quantum computing with Qiskit (2024)
- Jerbi, S., Gyurik, C., Marshall, S., Briegel, H., Dunjko, V.: Parametrized quantum policies for reinforcement learning. In: *Advances in Neural Information Processing Systems*, vol. 34, pp. 28362–28375 (2021)
- Liu, Y., Arunachalam, S., Temme, K.: A rigorous and robust quantum speed-up in supervised machine learning. *Nature Physics* **17**(9), 1013–1017 (2021)
- Meyer, N., Murauer, J., Popov, A., Ufrecht, C., Plinge, A., Mutschler, C., Scherer, D.D.: Warm-start variational quantum policy iteration. arXiv preprint arXiv:2404.10546 (2024)
- Meyer, N., Röhn, M., Murauer, J., Plinge, A., Mutschler, C., Scherer, D.D.: Comprehensive library of variational lse solvers. arXiv preprint arXiv:2404.09916 (2024)
- Meyer, N., Scherer, D.D., Plinge, A., Mutschler, C., Hartmann, M.J.: Quantum policy gradient algorithm with optimized action decoding. In: *Proc. 40th Int. Conf. Machine Learning (ICML)*, vol. 202, pp. 24592–24613 (2023)
- Meyer, N., Scherer, D.D., Plinge, A., Mutschler, C., Hartmann, M.J.: Quantum natural policy gradients: Towards sample-efficient reinforcement learning. In: *2023 IEEE International Conference on Quantum Computing and Engineering (QCE)*, vol. 2, pp. 36–41 (2023)
- Meyer, N., Ufrecht, C., Periyasamy, M., Scherer, D.D., Plinge, A., Mutschler, C.: A survey on quantum reinforcement learning. arXiv:2211.03464 (2022)

- Meyer, N., Ufrecht, C., Periyasamy, M., Plinge, A., Mutschler, C., Scherer, D.D., Maier, A.: Qiskit-torch-module: Fast prototyping of quantum neural networks. arXiv:2404.06314 (2024)
- Nielsen, M.A., Chuang, I.L.: Quantum Computation and Quantum Information: 10th Anniversary Edition, 10th ed. edn. Cambridge University Press, New York, NY, USA (2011)
- Packer, C., Gao, K., Kos, J., Krähenbühl, P., Koltun, V., Song, D.: Assessing generalization in deep reinforcement learning. arXiv:1810.12282 (2019)
- Periyasamy, M., Hölle, M., Wiedmann, M., Scherer, D.D., Plinge, A., Mutschler, C.: Bcqq: Batch-constraint quantum q-learning with cyclic data reuploading. arXiv preprint arXiv:2305.00905 (2023)
- Preskill, J.: Quantum computing in the NISQ era and beyond. *Quantum* **2**, 79 (2018)
- Rohde, D.L., Plaut, D.C.: Language acquisition in the absence of explicit negative evidence: How important is starting small? *Cognition* **72**(1), 67–109 (1999)
- Sutton, R., Barto, A.: Reinforcement Learning: An Introduction. MIT Press, Cambridge, MA, USA (2018)
- Skolik, A., Jerbi, S., Dunjko, V.: Quantum agents in the Gym: a variational quantum algorithm for deep Q-learning. *Quantum* **6**, 720 (2022)
- Sutton, R.S., McAllester, D., Singh, S., Mansour, Y.: Policy gradient methods for reinforcement learning with function approximation. *Advances in neural information processing systems* **12** (1999)
- Szegedy, C., Zaremba, W., Sutskever, I., Bruna, J., Erhan, D., Goodfellow, I., Fergus, R.: Intriguing properties of neural networks. arXiv:1312.6199 (2014)
- Tamar, A., Glassner, Y., Mannor, S.: Optimizing the CVaR via sampling. In: Proc. AAAI Conf. Artificial Intelligence (AAAI) (2015)
- Takase, R., Yoshikawa, N., Mariyama, T., Tsuchiya, T.: Stability-certified reinforcement learning control via spectral normalization. *Mach. Learn. Appl.* **10**, 100409 (2022)
- Wu, S., Jin, S., Wen, D., Han, D., Wang, X.: Quantum reinforcement learning in continuous action space. arXiv preprint arXiv:2012.10711 (2020)
- Wang, H., Zheng, S., Xiong, C., Socher, R.: On the generalization gap in reparameterizable reinforcement learning. In: Proc. Int. Conf. Machine Learning (ICML), vol. 97. PMLR, ??? (2019)
- Xu, H., Mannor, S.: Robustness and generalization. *Mach. Learn.* **86**(3), 391–423 (2012) <https://doi.org/10.1007/s10994-011-5268-1>
- Yun, W.J., Kwak, Y., Kim, J.P., Cho, H., Jung, S., Park, J., Kim, J.: Quantum multi-agent reinforcement learning via variational quantum circuit design. In: 2022 IEEE 42nd International Conference on Distributed Computing Systems (ICDCS), pp. 1332–1335 (2022)
- Yu, W., Tan, J., Liu, C.K., Turk, G.: Preparing for the unknown: learning a universal policy with online system identification. *Robotics: Science and Systems (RSS)* (2017)
- Zaman, K., Marchisio, A., Hanif, M.A., Shafique, M.: A survey on quantum machine learning: Current trends, challenges, opportunities, and the road ahead. arXiv preprint arXiv:2310.10315 (2023)